HHS Public Access

Author manuscript

J Cardiovasc Transl Res. Author manuscript; available in PMC 2017 April 01.

Published in final edited form as:

J Cardiovasc Transl Res. 2016 April ; 9(2): 102–118. doi:10.1007/s12265-016-9679-z.

CALCIFIC AORTIC VALVE DISEASE: PART 1 – MOLECULAR PATHOGENETIC ASPECTS, HEMODYNAMICS AND ADAPTIVE FEEDBACKS

Ares Pasipoularides, MD, PhD, FACC

Consulting Professor of Surgery, Duke University School of Medicine. Formerly, Director of Cardiac Function, Duke/NSF Research Center for Emerging Cardiovascular Technologies. Duke University, Durham, N.C. 27710, USA, Tel: 828-254-0279

Ares Pasipoularides: apasipou@duke.edu

Abstract

Aortic valvular stenosis (AVS), produced by calcific aortic valve disease (CAVD) causing reduced cusp opening, afflicts mostly older persons eventually requiring valve replacement. CAVD had been considered “degenerative,” but newer investigations implicate active mechanisms similar to atherogenesis—genetic predisposition and signaling pathways, lipoprotein deposits, chronic inflammation and calcification/osteogenesis. Consequently, CAVD may eventually be controlled/reversed by lifestyle and pharmacogenomics remedies. Its management should be comprehensive, embracing not only the valve but also the left ventricle and the arterial system with their interdependent morphomechanics/hemodynamics, which underlie the ensuing diastolic and systolic LV dysfunction. Compared to even a couple of decades ago, we now have an increased appreciation of genomic and cytomolecular pathogenetic mechanisms underlying CAVD. Future pluridisciplinary studies will characterize better and more completely its pathobiology, evolution and overall dynamics, encompassing intricate feedback processes involving specific signaling molecules and gene network cascades. They will herald more effective, personalized medicine treatments of CAVD/AVS.

Keywords

hemodynamics; aortic valvular stenosis (AVS); genomics of calcific aortic valve disease (CAVD); bicuspid aortic valve disease (BAVD); aortic valve inflammation; fibrosis and calcific nodule buildup; aortic transvalvular pressure gradient; intrinsic component of the total systolic ventricular load; pressure loss recovery; compensatory myocardial hypertrophy in pressure overload (PO); feedback control of myocardial hypertrophy; fetal type genes; immediate early-response genes (IEGs); replication of cardiomyocyte sarcomeres in-parallel and in-series; macromolecular crowding and cardiomyocyte diameters in PO hypertrophy

Compliance with Ethical Standards: Fully compliant

Ethical approval: All procedures performed in studies involving **human** participants that are reviewed here were in accordance with the ethical standards of the institutional and/or national research committee and with the 1964 Helsinki declaration and its later amendments. All applicable international, national, and/or institutional guidelines for the care and use of **animals** in studies involving animals that are reviewed here were followed.

I declare that I have no conflict of interest, whatsoever.

A lot of people spend their last decade of their lives in pain and misery combating disease—

Dr. J. Craig Venter

Δεινόν το γήρας, ου γάρ έρχεται μόνον Daunting is old age, for it never comes alone—

Menander, Greek poet and comedic author (342–291 BCE)

INTRODUCTION

Aortic valve stenosis (AVS) is the most common acquired valvular heart disease in the United States and western industrialized countries and is becoming more prevalent as the population demographics change, with an increasing proportion of the population over the age of 65. It is commonly expressed in old-age as degenerative tri-leaflet valve calcification, inasmuch as rheumatic disease is nowadays rare, and it is also referred to as age-related degenerative or dystrophic calcific AVS, and as calcific aortic valve disease (CAVD). Some 2% of the population have congenitally bicuspid aortic valves (BAV, see subsequent discussions), which are much more likely to calcify than tricuspid ones, and about 50% of these will develop CAVD [1–3]. The AV leaflets are made up of specialized valvular endothelial and interstitial cells akin to fibroblasts and an extracellular matrix (ECM) that contains collagen, elastin and glycosaminoglycans. Valve cells and the extracellular microenvironment are dynamic and reciprocally regulated; interstitial cells interact with their microenvironment directly via integrins, with biochemical signals through receptors, and with adjacent cells via cadherins [4, 5]. The valvular endothelium is an important regulator of (patho) physiological processes, including atherogenesis [6, 7].

MOLECULAR, GENOMIC AND HISTOPATHOLOGIC ASPECTS OF CAVD

CAVD had formerly been considered as a passive and nonmodifiable wear-and-tear disease process that comes with advancing age. However, considerable evidence has now accumulated from molecular studies supporting a cell-mediated active malady involving risk factors and histopathophysiological features (endothelial cell and macrophage activation, proteolytic activity, and osteogenesis in inflamed valves with similarities to skeletal bone formation) that characterize atherosclerosis [6, 8, 9]. It was probably Leonardo da Vinci (1452–1519) [10] who first recognized atherosclerotic macroscopic changes; when he illustrated arterial atherosclerotic lesions in an elderly man at autopsy, he attributed the thickening of the vessel wall to “excessive nourishment” from the blood [11]. Interestingly, Leonardo’s analysis of cusp geometry in relation to function identified the inherent mechanical advantage of a 3-cusp aortic valve. He concluded that 2 cusps would not allow a sufficient aperture for efflux of the blood, and that 4 cusps would be too weak in closure, and that the 3 cusps that nature prescribed were optimal [10]. In 1905, the eminent pathologist Johann Georg Mönckeberg first described CAVD in *Virchows Archiv*, as a passive process associated with rheumatic fever or aging [12].

The recognition that CAVD arises from active cellular mechanisms involving genetic and epigenetic interactions implies that the causative processes might be targeted to treat medically, which has clear-cut restorative implications.

Interaction of intrinsic programmed gene expression and local epigenetic factors

During the left ventricular (LV) pumping cycle, the aortic valve endothelium is subjected to complex fluid dynamic sways that are distinctly different on each side of the valve [13]. Intriguingly, endothelial phenotype is determined by a combination of intrinsic programmed gene expression and local epigenetic or environmental extrinsic factors [4, 5, 13]. Mechanical stresses on the cusps in conjunction with atherosclerotic risk factors can induce endothelial dysfunction/leakage with buildup of lipids and minerals, which provoke inflammation and actuate valvular myofibroblasts and/or circulating pluripotent mesenchymal cells resulting in their osteoblastic metaplasia/transdifferentiation [14]; these processes provoke ECM alterations and neovascularization [15]. Inversely, ECM composition and stiffness may, in turn, have a profound impact on the phenotype of valve interstitial cells, specifically fibroblasts, and ECM may contribute to their transdifferentiation to an osteoblast-like phenotype [16–18]. Leaflet collagen and elastin content commonly decline with age, and this is attended by an upregulated expression of elastolytic cathepsins and collagen-degrading matrix metalloproteinases—MMP-1 (fibroblast type collagenase), MMP-3 (stromelysin-1), MMP-9 (gelatinase B) and MMP-13 (collagenase-3); MMPs are strongly upregulated in CAVD and contribute to valvular remodeling and calcification [19–21].

Degenerative AVS is caused by an initial loss of collagen followed by calcification of the valve tissues leading to flow-associated turbulence beyond the orifice [13] and an “atheroprone” hemodynamic environment of increased turbulent shear stresses and stretch applied on the valve cusps. This furthers inflammation and extracellular matrix remodeling and may contribute to early localization of the sclerotic valve calcification preferentially in the fibrosa, the interstitial layer on the aortic side (outflow surfaces) of the leaflets—cf. small inset depicting the calcific nodules, in Figure 1. An early, fluid dynamically insignificant stage of minor (cusp-tip) calcification is known as aortic valve sclerosis; its prevalence increases with age and it has a low rate of progression to AVS, but it can be significantly correlated with a compounded risk of coronary events, stroke, and cardiovascular mortality [22].

Turbulence begets further collagen loss and tissue mineralization of the valve, scarring, and thickening that stiffen the leaflets (decreased pliability) and can lead to progressive narrowing of the valve opening with a significant increase in transaortic jet velocity and hemodynamic impediment. Recent findings indicate the development of highly heterogeneous, heavy hydroxyapatite—$Ca_5(PO_4)_3OH$—deposits within the calcific aortic valve tissues, leading to bone-like, rigid calcific nodules [23]. They suggest a gradual maturation process with changes in the composition of the valvular tissue akin to the multistep development of bone tissue during intramembranous ossification in the skull, where mesenchymal cells proliferate and condense to produce osteoblasts, which deposit a

collagen-proteoglycan osteoid matrix that is able to bind calcium into compact nodules [24, 25].

Metabolic factors connected with CAVD histopathology

The changes characterizing CAVD are actually brought about by a highly structured, dynamic and extensively regulated chain of inflammation, fibrosis and dystrophic calcification (not caused by hypercalcemia), which can result in gross leaflet thickening and induration with nodular atherocalcification and immobility encumbering opening. As the disease progresses, lipid, inflammatory cells, and extracellular matrix are increased and there is breakdown and displacement of the elastic lamina [26]. There is direct molecular imaging evidence indicating that CAVD entails mechanisms similar to those involved in osteogenesis (Gk: bone formation) [27]. If untreated, CAVD progresses successively through secondary LV hypertrophy (Gk: increased growth), symptom development (angina, dyspnea on exertion, fatigability, fainting with exertion, heart palpitations), and ensuing decompensation with transition to heart failure [28]. After nodular calcium accretions grow within the valve, reversibility becomes uncertain; nevertheless, inflammation, neoangiogenesis, and early valvular ECM remodeling changes portending significant fibrosis and calcific nodule buildup may still overlap an applicable therapeutic window that precedes potentially irreversible fibrosis and ossification. Currently, late stages of CAVD are treated surgically, because no medical treatments exist *yet* to reverse, slow, or halt advanced disease aftermaths.

Actually, a genetic susceptibility toward elevations in low-density lipoprotein cholesterol, but not in high-density lipoprotein (HDL) cholesterol or triglycerides, is connected with the manifestation of aortic valve atherocalcific changes and the occurrence of CAVD [29] ; moreover, it has been shown that lowering plasma cholesterol levels halts progression of aortic valve disease in mice [30]. Patients with visceral obesity [31] have low HDL levels with elevated levels of circulating low-density lipoprotein (LDL); the small and dense LDL particles have a higher ability to infiltrate the aortic valve and are quickly transformed to oxidized LDL owing to the low HDL levels with a reduced anti-inflammatory activity. Inflammatory cells are then attracted within the aortic valve and macrophages are stimulated by oxidized LDL to turn out cytokines such as tumor necrosis factor (TNF)-alpha, which promotes an osteoblast-like phenotype in human aortic valve myofibroblasts [32]; osteoblast differentiation processes in CAVD with or without BAVD (see below) are also mediated by the Lrp5/Wnt3 pathway [33]. Remarkably, interleukin-6 (IL-6) mediates the mineralization of the aortic valve, although in bone it activates osteoclastogenesis, the development of *osteoclasts*—Gk: bone-breaker, a type of bone cell that *breaks down* bone tissue [34]. Epidemiological data show that in humans too statin therapy is associated with slowing of the hemodynamic progression of CAVD [35, 36]. Nevertheless, there is controversy and conflicting reports too [37–40], suggesting that additional unknown factors may well contribute to the progression of CAVD.

BAV disease particularities

Plausible explanations for the aforementioned (see **INTRODUCTION**) higher prevalence and earlier-onset CAVD in BAV patients include the abnormal fluid dynamic stress and

strain patterns sustained by the cusps, which may initiate/accelerate the biopathologic processes of CAVD; alternatively, the genomic variants that underlie BAV may result in CAVD, more or less independently of the associated fluid dynamic disturbances. BAV disease (BAVD) has a strong genetic basis and may accompany many other congenital cardiovascular defects including coronary artery anatomic anomalies, aortic coarctation, patent ductus arteriosus, ventricular septal defects, and Marfan syndrome [41]; however, the precise causes and intricate interactions that may implicate signaling pathways of BAV calcification and aortic root dilatation, as well as the multiscale interconnected effects of valvular calcification, hemodynamics, and aortic medial degeneration remain unknown.

Turbulent flow disturbances and ascending aortic dilatation are common in BAVD, even in absence of significant aortic stenosis or regurgitation. The aortopathy of BAVD is attended by cystic medial degeneration, variations in signaling pathways and matrix metalloproteinase activity and by apoptosis [4, 5], thus putting the patient with BAV at increased risk for aortic aneurysm and dissection—such complications can cause problems during and after aortic valve replacement. Combining the various new tools for discovery, as developed in subsequent Sections of this Survey, promises to yield burgeoning insights into the genomic underpinnings of BAV and CAVD.

Genome-wide association studies of CAVD

Up to now, investigations into genetic risk factors underpinning disease susceptibility to CAVD may have examined data from large numbers of patients but while focusing on only a small number of gene variants, one at a time. New proteomic approaches that entail genome-wide association studies (GWAS) [41–43] sequencing both haploid genomes of individuals should identify genomic variations, such as loci of common single-nucleotide polymorphisms (SNPs) [41, 43] across the genome, and correlate them with susceptibility to CAVD and severity of AVS, with the ultimate goal of defining causal genetic pathways and molecular mechanisms [44]. I have examined difficulties and caveats of such studies of multifactorial diseases recently [41]; they pertain primarily to the fact that expressed traits/phenotype are the outcome of primary causal mutations/variants, of modifier genes ushering into the picture gene–gene interactions (GxG), and also of environmental factors contributing gene–environment (GxE) interactions. Once we identify diverse pathobiologic mechanisms controlling why certain individuals develop CAVD, while others live well into old age without expressing it, we may be in position to identify rational targets for the development of small molecule, gene transfer, or cell-based therapies to prevent or retard the progress of CAVD and to customize such treatments as needed in variously susceptible individuals—personalized medicine!

DIAGNOSTIC ASSESSMENT

In the diagnostic evaluation of the patient with CAVD/AVS, examination of all four cardiac valves and checking for other lesions that might be mistaken for aortic valvular disease are important; e.g., other diagnostic possibilities might include a subaortic membrane, mitral regurgitation, ventricular septal defect, and hypertrophic cardiomyopathy [13, 41, 54, 62, 74, 79, 83, 87]. A thorough examination encompasses exclusion/confirmation of each

differential diagnosis, as well as the appraisal of the aortic valve itself. Echocardiography, cardiac computed tomography (CT), magnetic resonance imaging (MRI), and positron emission tomography (PET) each offer advantages and disadvantages, and sometimes at least two modalities are needed to get comprehensive, accurate data.

Echocardiography

Asymptomatic patients with suggestive murmurs at screening auscultation benefit from early diagnosis, which can guide the use of prophylactic regimens to prevent bacterial endocarditis. Echocardiography (transthoracic, complemented with transesophageal 3D ultrasound [45] that allows better visual appreciation of the evolving morphology of calcific nodular deposits) is the primary noninvasive imaging modality used to diagnose and manage severe AVS. It is valuable for serial examinations, in identifying appropriate patients for surgical/percutaneous interventional procedures, in permitting interventional intra-procedural guidance and for convenient post-procedural follow-up for early detection of complications [46–48]. 3D echocardiographic orifice area measurements are more accurate than either with 2D planimetry or the continuity equation (see below), because 3D makes possible exact *en face* alignment of the cut planes to the valve allowing reliable and straightforward identification of the narrowest area [13, 45, 49].

Quantitation of valvular thickness is constrained by the technical characteristics of ultrasound, but an evaluation of leaflet structure, reflectance, and mobility when feasible, is desirable. Nodular thickening of one or more of the aortic cusps is an early echocardiographic sign of age-related degeneration and CAVD; the thickening is usually located in the vicinity of the nodule of Arantius or at the base of the commissures. The ultrasound-based imaging evaluation of myocardial deformation related parameters provides efficient insights into myocardial dynamics in patients with CAVD and can supply wide-ranging and robust information for monitoring LV systolic and diastolic properties and function.

Strain echocardiography allows objective assessment of myocardial mechanics and of segmental and global LV systolic performance; evaluation of longitudinal (LS), radial (RS) and circumferential (CS) LV myocardial strains is accurate and reproducible [50]. Doppler tissue imaging (DTI) and speckle tracking echocardiography (STE) have shown that *pathological* LV hypertrophy leads to increased LV mass with most patients displaying depressed LS, CS and RS [51]. Contrariwise, *physiological* hypertrophy in endurance athletes presents enhanced LS, CS and RS values, with preserved or enhanced LV systolic and diastolic performance. Moreover, endurance exercise training may delay age related deterioration of LV longitudinal function [52]. These echocardiographic findings distinguish pathological from physiological hypertrophy (see Section on Contrasting Physiological and Pathological Cardiac Hypertrophy in the companion Part 2 of this Article); however, studies on the effects of endurance training on rotational mechanics (LV torsion, or twisting and untwisting [53, 54]) have shown conflicting results. 2-Dimensional (2D) and 3D Doppler velocimetry are suitable means both for gauging the severity of AVS by measuring orifice jet velocity and pressure gradients—a mean gradient ≥ 30 mm Hg usually represents clinically

significant aortic stenosis—and for estimating the aortic valve area by applying the continuity equation [13, 45, 55–61].

Cardiac catheterization

Although there is no longer a “routine” cardiac catheterization, in cases in which the echocardiographic estimates are not in line with clinical findings, cardiac catheterization is advocated for a definitive hemodynamic evaluation [13, 62, 63]; diagnostic interventions made in the catheterization laboratory include the use of dobutamine in low-flow states, and exercise hemodynamics. Hemodynamic catheterization needs to be done with meticulous attention to detail and performed by persons with knowledge and expertise [63]. However, pressure gradient in AVS may be misleading in patients with poor LV function.

Because of their strong dependence on applying flow rates (see Fig. 2) [13, 64–68], high transvalvular pressure gradients are contingent upon adequate cardiac output and absence of severe LV systolic dysfunction; obversely, the gradient is 0 when there is no cardiac output. While aortic valve replacement is generally justified if severe AVS is proved, patients with primary LV myocardial dysfunction and a resulting diminished aortic valve opening do not benefit from valve replacement [69]. Distinguishing between the two situations is necessary but not possible with echocardiography at rest. Pseudo-severe AVS, in which a non-severe stenosis seems severe because of concomitant LV dysfunction from other causes resulting in low flow and consequently a reduced valve opening, can be reliably verified/ruled out by applying positive inotropic stimulation with dobutamine stress echocardiography [70, 71].

Conversely, patients with low LV ejection fraction (LVEF) but resting peak aortic velocity ≥ 4.0 m/s or mean transvalvular gradient ≥ 40 mm Hg do not actually have LV systolic dysfunction as the apparently reduced LVEF in these patients is only a consequence of the high afterload, and LV function and EF are likely to rise after relief of the severe stenosis with outflow obstruction. The majority of all patients with severe AVS and LV systolic dysfunction belong to this category. The transvalvular gradients are exaggerated in settings of elevated cardiac output (e.g., exercise, anemia, serious sepsis) [13, 72]. Aortic valve area planimetry by transesophageal 3D echocardiography affords an anatomic measurement; there is, however, a strong “*orifice*” *shape*-dependence of the ratio of anatomic/effective valve area, and also of the coefficients A and B in Eq. 1 (unsteady Bernoulli equation; see next Section).

CT, MRI, PET and Combined PET/CT

Because of the requirement for ionizing radiation and radiocontrast agents, computed tomography (CT) has a restricted role in the diagnosis, serial assessment and surveillance of AVS/CAVD as primary indication. It may sometimes be employed as such if echocardiographic results are inconclusive and there are contraindications for magnetic resonance imaging (MRI) (http://www.mrisafety.com/TheList_search.asp). Nevertheless, with the introduction of subsecond rotation coupled with multi-slice CT (up to 320-slices), high speed and high resolution can be achieved together, permitting first-rate imaging of the coronary arteries (cardiac CT angiography). Accordingly, CT use for noninvasive coronary angiography is increasing, and advantageous information on valve anatomy and function can

be acquired alongside a coronary examination. In more sophisticated applications, CT with PET can be used to provide even more detailed, reproducible, and accurate assessment of the calcific burden along with spatiotemporal displays of the calcific processes occurring within the valve [73].

Combined PET/CT is a high-tech, noninvasive, reliable diagnostic method for measuring the degree of valve inflammation and calcification in CAVD. It combines functional data from PET with delineated anatomical information from CT. Thus, fused PET/CT images on the same gantry allow quasi-simultaneous image acquisition to localize specific biochemical/pathobiologic processes to individual structures. In principle, any biochemical process can be investigated, utilizing a suitable PET tracer, consisting of a positron emitter, such as Carbon-11 (^{11}C), Nitrogen-13 (^{13}N), Oxygen-15 (^{15}O) and Fluorine-18 (^{18}F), produced within a medical cyclotron and attached to molecular agents that target the biochemical process concerned. This approach affords a potential method for gauging CAVD pathobiologic activity (e.g., inflammatory signaling in CAVD), which might then allow prediction of disease progression and could serve to identify proxy endpoints in investigations/trials of innovative therapies, capable of modifying disease progression.

TRANSLATIONAL FLUID DYNAMIC FOCUS ON AVS

Hypertrophy is a morphomechanical cardiac adaptation to an increased workload. As physiological hypertrophy, occurring during pregnancy or with exercise training, is characterized a hypertrophic response associated with preservation of LV function. In contrast, a pathological hypertrophy as occurs with CAVD is a hypertrophic response that predisposes to or progresses to heart failure. Exactly how is pathological differentiated pathogenetically from physiological cardiac hypertrophy? This riddle persists as an important question in basic cardiovascular research with clinically far-reaching translational repercussions. The comprehensive solution to the enigma will be most illuminating and fruitful in understanding and managing pathogenetic processes/stimuli and the molecular derangements underlying hypertrophic heart disease and possible heart failure arising in response to CAVD. In recent years, the influence of the nature of pathogenetic hemodynamic factors/stimuli on the development of cardiac hypertrophy can be evaluated effectively with high-fidelity instrumentation for measurements on human patients and experimental animals [13].

In perspicaciously examining hemodynamic measurements, one should keep in mind some important facts, as follows: Fluid dynamic principles previously discussed in detail [13, 62, 75, 77–79, 84–86], show that ejection should be associated with considerable pressure gradients and intraventricular and transvalvular pressure differences, even in the absence of obstruction. At times, multisensor catheter gradients measured by micromanometers 5 cm apart in normal subjects may transiently exceed 25 mm Hg (or 5 mm Hg/cm) during submaximal (5–6 METs) supine ergometric bicycle exercise. As aortic valvular stenosis develops, the maintenance of adequate levels of LV output requires progressive obligatory increases in linear velocity through the narrowed valve. Peak linear velocities in excess of 5 m/s (vs. ≈ 1 m/s normal) can be attained in the vicinity of the stenosed orifice and beyond, in the jet of turbulent flow at the aortic root. Because representative velocities in the deep

chamber are of the order of 0.1 m/s, it follows that, compared with normal, strong intensification of convective acceleration effects (occurring when the flow is non-uniform, i.e., if the velocity changes with position along the flow) takes place in the subvalvular region of the ejecting chamber (see Fig. 3). This accounts for the strikingly accentuated ejection pressure gradients that are quantified by the unsteady Bernoulli equation, as will be shown below.

Moreover, there are not only quantitative but also *qualitative* differences between obstructive and nonobstructive ejection gradients, just as there is a fundamental dissimilarity between accelerating a fluid by means of a piston in a uniform tube and accelerating it by means of a constriction. Accordingly, proper interpretation of systolic physiological and pathological ejection pressure gradients requires much more information than simply their magnitude. Consider the fluid dynamics of ventricular outflow orifice stenosis. The large obstructive micromanometric pressure gradient tends to be quite symmetric and "rounded" and closely tracks the ejection flow waveform, as does the characteristic *crescendo-decrescendo* high-frequency murmur. This large gradient is, in fact, associated with a relatively low peak volumetric outflow rate recorded simultaneously at the aortic root. It is the greatly augmented contribution of the convective acceleration, or Bernoulli, component (see below) to the total measured systolic pressure gradient in aortic or pulmonic stenosis that causes it to be more *in-phase* with the ejection velocity than is seen normally. As previously emphasized [13, 62, 74], this is equally as important a hemodynamic hallmark of severe aortic stenosis as the augmentation of the magnitude of the driving pressure gradient.

The greatly amplified *intrinsic* (intraventricular) portion of the *total* systolic load

Figure 3 encompasses in a nutshell salient fluid dynamic aspects of AVS. A left-heart catheter with two laterally mounted solid-state micromanometers, one at the catheter tip and the other 5 cm proximally, was used to obtain the tracings; an electromagnetic velocity probe was mounted at the level of the proximal micromanometer. In the top panel A, both micromanometers are deep in the chamber, and a barely discernible pressure "gradient" is associated with the small, slowly rising, deep-chamber velocity waveform. The substantial energy needed to accelerate the outflow across the stenotic valve opening is revealed by the large systolic pressure drop between the deep LV chamber and the vicinity of the orifice (top panels B & C), and reflects the greatly increased *intrinsic* component of the *total systolic load*, according to the theory that I have formulated and applied in previous publications [13, 62, 74–78].

In the third beat of panel B of Figure 3, the downstream micromanometer and the velocimeter are in the immediate vicinity of the stenosed orifice, and the measured gradient is increased along with the velocity. Interestingly, in the third beat of the panel, where the velocity is highest, the downstream pressure exhibits a prominent *mid-systolic dip* coincident with *peak velocity*. Such a "dip" requires meticulous effort to be demonstrated in aortic stenosis, although a large-scale counterpart is typically present in micromanometric recordings from the outflow tract or the aortic root in cases of hypertrophic cardiomyopathy with large dynamic systolic gradients [13, 41, 62, 79]. This is a good example of the important, albeit subtle, hemodynamic measurement findings and insights that are within the

province of the translational cardiologist with requisite preparation in and understanding of cardiac fluid dynamics, while appearing to be “accidents” without apparent cause and void of any significance for the more casual observers.

As is detailed elsewhere [13, 62], it is my view, based on fluid dynamic analytic considerations and experience with micromanometric/velocimetric human catheterization data with and without outflow obstruction, that such a “dip” represents an unmistakable hallmark of intensified convective acceleration effects. In the aortic stenosis tracing in Figure 3B, note that the instantaneous pressure gradient is maximum at the inscription of the mid-systolic dip, right at the time when the velocity and its square attain their peak values; this is exactly as required by a flow process dominated by convective acceleration effects according to the unsteady Bernoulli equation. Alternatively, the dip can be viewed as a reflection of the transformation of ventricular flow work or “pressure energy” into the kinetic energy of the flow through the converging field of the stenosed orifice. Setting aside simple hydrostatic effects, the unsteady Bernoulli equation for the instantaneous pressure drop across an axial segment Δs, in terms of the applying flow rate, Q, and its rate of change with time, t, is as follows [13, 62, 75] :

$$\begin{array}{ccccc} \Delta P\,(s,\ t) & = & A\cdot \partial Q_r/\partial t & + & B\cdot (Q_r)^2 \\ \text{Total} & & \text{Local} & & \text{Convective} \\ \text{instantaneous} & = & \text{acceleration} & + & \text{acceleration} \\ \text{pressure drop} & & \text{component} & & \text{component} \end{array} \quad \text{[Eq. 1]}$$

Here, A and B are integration coefficients depending both on the applying instantaneous ventricular chamber geometry and the outflow “orifice”/opening shape, as well as on the shape of the ejection velocity curve; s denotes axial coordinate, and the subscript r signifies a reference position (for example, the aortic ring) for measurement of the volumetric flow rate, Q_r. Q represents the flux of axial velocity through a flow cross-sectional area; the time derivative $\partial Q_r/\partial t$ can be derived from the Q_r curve by numerical time-differentiation.

In the top C panel of Figure 3, the proximal pressure sensor is lodged in the aortic root and records the characteristically slow-rising, highly asymmetric, aortic stenosis pressure waveform in systole. This sensor and its companion electromagnetic velocity probe are slightly downstream of the obstruction, within the jet issuing from it. Highest velocity signals are recorded along with maximal peak instantaneous and mean transvalvular pressure gradients. It is these maximal values of orifice velocity and pressure drops that should be used to assess *effective orifice area* by both invasive and noninvasive methods [13].

Pressure loss *recovery* across the aortic valve

Compare now the pressure tracings in the top C and D panels of Figure 3: in D the downstream sensors for pressure and velocity are in the region of turbulent flow in the post stenotic dilatation of the ascending aorta. Note that the downstream pressure in D has *recovered* very markedly from its levels in C in conjunction with the decrease in the linear velocity and hence the kinetic energy of the flow, as required by the Bernoulli equation.

Thus, although the upstream micromanometer in D still records deep LV pressure levels unchanged from those of panels A, B, and C, the downstream one records much higher systolic pressures in D than in C. In the example illustrated, the peak-to-peak pressure gradient is lower by about 20 mm Hg in panel D than in panel C, as a result of the equal (20 mm Hg) *increase* in the peak downstream pressure. These considerations explain why echocardiographically derived orifice areas in AVS yield higher effective transvalvular pressure gradient levels compared with those measured at catheterization.

Catheters used in clinical practice measure pressure in the proximal aorta, downstream from the aortic valve and beyond where (a variable) pressure loss recovery has ensued. The downstream pressure can recover very markedly in conjunction with the decrease in the linear velocity and hence the kinetic energy of the flow, as required by the Bernoulli equation. However, echocardiographic calculation of stenosed orifice area by the continuity equation uses the highest velocity of the aortic jet in the vena contracta, upstream from where pressure recovery comes about. The vena contracta is the smallest region of the aortic outflow with highest velocity jet and is typically located at or just downstream from the stenosed orifice. Accordingly, orifice area obtained by echocardiography corresponds to a higher effective transvalvular pressure gradient than that measured by multisensor left-heart catheter.

Such practical translational considerations led me to introduce in the cardiovascular literature in 1990 the intriguing phenomenon of pressure loss recovery in my survey on "*Clinical Assessment of Ventricular Ejection Dynamics With and Without Outflow Obstruction,*" in *JACC* [62]. As has been noted in the international literature [80–82], pressure loss recovery was a previously unrecognized/unreported catheterization finding at the time that I presented in that seminal paper analytical reasoning and the first micromanometric-velocimetric multisensor catheter tracings (cf. panels A, B, C, D of Fig. 3) demonstrating it in the ascending aorta of patients with AVS [62].

As I further pointed out in that survey and elsewhere [13, 62], if reduced volumetric velocities and accelerations did not prevail in AVS, the LV ejection pressures in severe cases would have to rise to levels unattainable even with very thick walls. This would occur irrespective of turbulent jet losses downstream of the stenosed valve, and despite normal or subnormal aortic root pressure levels. It is ascribable to the fact that the convective acceleration component in the subvalvular region of the outflow tract and through the vena contracta (Fig. 3) increases in proportion to the square of the velocity. Contrary to conventional thinking, it is not "turbulent valve losses" that account for the great augmentation of ventricular load in aortic stenosis. Viscous dissipation in the separated turbulent flow beyond the stenosed valve simply accounts for the incomplete recovery of static pulsatile pressures as stream cross-section reexpands distal to the stenosis. As previously commented [13, 62], such turbulent dissipation of kinetic energy downstream of the stenosed valve actually *spares* the systemic arteries from the ravages that would be associated with the substantial recovery of abnormal LV systolic pressures in excess of 200 mm Hg, which are needed to rapidly force ejection through the strongly confluent subvalvular flow field (cf. Fig. 3).

In the context of the preceding paragraphs, it is imperative that, during the catheter pullback procedure, one should keep in mind that if the upstream (intraventricular) micromanometer is located within, or even very near, the subvalvular region of the LV chamber, the pressure gradient measured by a “double-tip” micromanometric catheter withdrawn through the orifice will progressively decrease not only because of the pressure loss recovery affecting the downstream micromanometer, but also because of a fall in pressure at the upstream sensor. This is a consequence of the fact that most of the convective pressure drop occurs in the subvalvular region, where the convective acceleration effect during ejection is most intense [13, 62, 83–87]. This tremendously important fact is strikingly demonstrated in the bottom panel of Figure 3: The solid-state multisensor catheter pullback reveals that the “transvalvular” pressure gradient is, practically in its entirety, *intraventricular* in origin and accrues in the subvalvular region of the chamber—cf. the “magnifying lens” inset in Figure 3.

FEEDBACKS ACTUATED BY CAVD-INDUCED PRESSURE OVERLOAD

Evidently, AVS-induced mechanical alterations in the LV myocardial “environment” may have serious pathophysiological and clinical consequences following their mechanotransduction by myocardial and, presumably, by autonomic neural cells [88]. Mechanotransduction contributes to cardiac function by initiating time-related adaptive myocardial cell and ECM morphomechanical adjustments [4, 5, 13]. As is true of other homeostatic mechanisms, mechanotransduction can be viewed as a feedback control loop initiator with vital clinical relevance, considering that it transduces forces into sarcomerogenesis (cf. Fig. 1) that can bring about cardiomyocyte thickening and/or lengthening. It can either stabilize, through negative feedback loops, or destabilize, through components exhibiting positive feedback, the dynamics of the system (see Fig. 4), demonstrating nonlinear complexity as do most integrative physiological processes [13]. Here “positive” and “negative” do not ascribe a positive or negative final effect to the consequences of the feedback, nor do they refer to desirability of outcome.

Feedback delays

Negative feedback mechanisms, all operating in parallel, maintain within normal range basic physiological parameters of cardiomyocyte function. Negative feedbacks entail end-product/end-state activation and inhibition processes in which sustained deviations from target values, which represent steady-state operating levels of ventricular/cardiomyocyte function, lead to compensatory changes after a time lag that can be hard to optimize/curtail. Although negative feedback loops in which just the right amount of correction is applied with optimum timing can be very stable, accurate, and responsive, system oscillation is the characteristic symptom of physiologic negative feedback configurations in which the information used to take goal-seeking action is delayed. In such circumstances, the control action is not based on the current state of a system but on some previous state or value. Obviously, using dated information to control the approach to a target level is likely to cause the system to miss, overshoot or subsequently undershoot, its goal.

Excessive stretching of cardiomyocyte components by too high developed systolic sarcomeric stresses in AVS-provoked pressure overload (PO) induces expression of specific genes, such as immediate early-response genes (IEGs) and fetal type genes [89, 90]. IEGs are genes that are activated transiently and rapidly in response to stretch or increased developed contractile tension. They represent a readily available response machinery that is activated at the transcription level in the first round of response to the feedback stimuli, before any new sarcomeric proteins are synthesized. The IEGs are distinct from "late response" genes [91], which can only be activated later, i.e., *following* the synthesis of early response gene products. In view of these adaptive responses, the PO-associated increased sarcomere and cardiomyocyte stretch and developed tension can in due course bring about augmented myocyte transverse diameters and LV wall thickness (see Fig. 1) to cope with the AVS-induced overload.

Information delays are prevalent in adaptive physiological control, so it is no surprise that oscillations are not uncommon. End-product/end-state activation and inhibition (see Fig. 4A) require a type of feedback control that operates *after* the protein synthesis involved in sarcomerogenesis has taken place. The transcription factors regulating activation/repression of sarcomeric protein genes quite naturally must enter the nucleus in order to exert any effect on the genomic DNA. Since they are translated, like most other proteins, in the cytoplasm they must cross the nuclear membrane to reach the chromatin, site of their action. Plainly, numerous reactions and translocations must transpire between the time that the actuating feedback signal is transduced and transmitted to the nucleus where transcription takes place —to be subsequently complemented by cytoplasmic ribosomal translation—and the time that the resulting sarcomeric protein molecules come to be fully formed, mature, and inserted in-place within the hypertrophying cardiomyocyte sarcomeres (see Fig. 1). Accordingly, feedback activation and inhibition encompass time delays of gene expression and adjustment implementation; these embody finite times for transduction, nuclear transmission, transcription, transcript splicing and processing, cytoplasmic translocation and protein synthesis, etc. [4, 5, 13, 41]. They can, therefore, result in oscillatory behavior of the "level" of the controlled system variable, viz. the stress demonstrated in Figure 5.

Transcriptional and allied delays can consequently drive oscillatory gene expression in regulatory gene networks. Furthermore, a variety of transcription factors—each of which is a component of a feedback activation/inhibition loop—have been observed to display oscillatory dynamics wherein their own intracellular levels vary periodically with time [92]. There is also a connection between the oscillation of gene expression and feedback adjustments relating to protein and mRNA half-lives—and mRNA levels can, in turn, be altered by faster/slower degradation or by increased/decreased transcription, and protein by degradation and translation (and indeed mRNA level).

The foregoing considerations help explain the oscillatory/undulating wall stress time course over the 40-week long banding period that is displayed in Figure 5. It is stimulating to think that already in the mid-1950s Dr. Arthur Guyton and his collaborators[93] at the University of Mississippi Medical Center demonstrated in canine experiments the basic oscillatory mechanism of Cheyne-Stokes breathing, which they elicited simply by increasing the circulation time from the oxygenation of blood in the lung to the stimulation of

chemosensitive sites in the brainstem, by introducing a plastic tube—time delay—in the carotid artery.

Negative feedback mechanisms

A negative feedback loop tends to slow down an evolving process, while a positive feedback loop tends to accelerate it; in a negative feedback reaction the system responds in such a way as to counteract the direction of change (see Fig. 4 A). Such a reaction is exemplified well by the compensatory myocardial hypertrophy that reduces/returns rising systolic LV wall stresses to normal levels in advancing AVS. It is a form of circular causality tending to maintain a stable state; to be exact, it is a tendency to diminish or counteract change allowing the maintenance of physiologic homeostasis under changed operating conditions (Fig. 4A) [13]. However, (mal) adaptive hypertrophy commonly compromises ventricular diastolic function [53, 98–100]. Excessive wall hypertrophy resulting in subnormal wall stresses at given diastolic pressures is accompanied by increased muscle stiffness and impaired relaxation dynamics, although the rate of force development and peak active force may not be impaired [53, 94–100]. The advanced age in CAVD patients is accompanied by attendant comorbidities, such as coronary heart disease, which by themselves can bring about myocardial ischemia and diastolic abnormalities; these can act synergistically to exacerbate the diastolic impairment [13, 78, 98–100].

LV hypertrophy in response to *pulmonary artery* banding (PAB) is an intriguing phenomenon [100–102], which may be associated with augmented generalized adrenergic stimulation affecting both ventricles; such an enhanced generalized activation of cardiovascular adrenergic receptors may also account for elevated systemic resistance levels found in pulmonary arterial banded dogs [100, 103]. For pulmonary arterial banding-induced pressure overload hypertrophy, Figure 5 demonstrates that mechanical properties (muscle stiffness) are markedly altered before substantial increases in wall mass are observed. Most notably, however, distending LV wall stress clearly exhibits a biphasic/undulating time course over the 40-week long banding period: it rises early to a maximum level (arrow at maximum in Fig. 5), then decreases gradually to normal and subnormal levels (arrow at minimum in Fig. 5), as a consequence of the increasing thickness of the hypertrophying walls; it eventually increases again as the ventricle dilates with ensuing late decompensation and failure. The underlying negative feedback systems are definitely subject to oscillations caused by inherent delays around any feedback loop. Such a decaying oscillatory/undulating behavior is, as we have seen, characteristic of processes involving typical negative feedback. Similar behavior was found to simultaneously apply also for the right ventricle of the PAB dogs [100].

The narrow distribution of cardiomyocyte diameters in PO hypertrophy, and “macromolecular crowding”

The expression of a stable and narrow distribution of cardiomyocyte diameter/size in AVS-induced PO hypertrophy suggests cell-autonomous negative feedback(s) controlling size variability. Indeed, contemplation of the striking homogeneity in cardiomyocyte diameter in the hypertrophic myocardium brings in focus the obvious need for an inhibitory (negative) feedback linking the growth rate of sarcomeres—being replicated in-parallel (Fig. 1)—to the

cardiomyocyte diameter. Such feedback inhibition might function by cardiomyocyte width-dependent sarcomeric protein degradation and/or other regulatory motifs acting to lessen cell-to-cell diameter inconsistency. In addition, negative feedbacks and reciprocal interactions between cardiomyocyte transverse diameter growth and tissue mechanics might be an important part of the hypertrophy process: growth and tissue mechanics cannot be studied in isolation. A general principle of how mechanics influence growth might be that the more cells are compressed transversely, the slower they grow/widen; conversely, when local differences of transverse growth occur, it is the faster-growing cells that are compressed more, curtailing their growth. It then comes to pass that the aforementioned reciprocal interactions result in a negative feedback on transverse diameter expansion, such that neighboring cell growth differences tend to be restricted.

Macromolecular mechanisms underlying these operational feedbacks need to be characterized in future studies. Sarcomeric macromolecules exist and work in an exceedingly structured and complex environment within the cardiomyocyte (endoplasmic reticulum, Golgi apparatus, cytoskeletal macromolecular assemblies/structures, etc). Complicating the picture further, the cell interior is not merely a crowded medium, but rather an utterly crowded and confining one. Cardiomyocytes contain a lot of big molecules, especially structural (such as the giant protein, titin—Fig. 1) and contractile proteins, comprising not only actin, myosin, tropomyosin, and troponins, but also other proteins that stoichiometrically bind to the core components and regulate cycling [104, 105], enzymes and nucleic acids; macromolecules develop and function within sarcoplasmic environments that are crowded with other macromolecules.

The very high total concentration of these molecules, or “macromolecular crowding” [106], has multifaceted consequences that could have an impact on many aspects of cellular growth, culminating in replication of sarcomeres in-parallel (see Fig. 1). Thus, the effect of volume occupancy on available volume is sensitive to the numbers, relative sizes and shapes of the molecules already present/produced. Undercrowded conditions should promote/accelerate macromolecule generation and/or inhibit macromolecule degradation. On the other hand, reactions/processes that increase the available volume should theoretically be promoted by crowded/confining conditions; such processes would include the inhibition of macromolecule generation and/or augmentation of their degradation, the binding of macromolecules to one another, the formation of aggregates, and the folding of protein and nucleic-acid chains into more compact shapes [107–109].

Positive feedback mechanisms

In positive feedback, the response is to amplify the incipient change. Positive feedback is another mode of circular causality, which—contrary to negative feedback—acts as a growth-generating mechanism (see Fig. 4B); i.e., the deviation of the system may grow persistently larger, displaying an unbounded response, or it may tend asymptotically toward a new value, exhibiting a bounded response. Such responses are exemplified, respectively, by the required progressive increase in contractile systolic stress per cardiomyocyte sarcomere with advancing PO in worsening AVS (Fig. 4B, *unbounded* response), and by the concomitant myocardial ECM fibrosis (Fig. 4B, *bounded* response) [13]. They typically have a

destabilizing effect and are maladaptive, so they disturb homeostasis and represent an induced departure from some antecedent normal state.

RECAP AND PROSPECTS

AVS brought about by calcification leading to incomplete cusp opening is the most frequent cardiac disorder, after coronary artery disease and systemic hypertension. It occurs mostly among older persons, who as it happens are commonly at high estimated surgical risk; TAVR is applied in such patients with severe symptomatic AVS. Historically, CAVD had been thought to be “degenerative,” the result of aging and wear of the aortic valve. This old paradigm has lost currency over the past quarter-century because of studies demonstrating that CAVD is actively mediated, with many mechanisms similar to those operative in atherogenesis. CAVD is commonly connected with systemic arterial mural histomechanical abnormalities resulting in diminished arterial compliance and holds numerous histological and molecular biological similarities to atherosclerosis, since their pathogenesis implicates signaling pathways and genetic predisposition, lipoprotein deposits, chronic inflammation and calcification/osteogenesis. This fact has a corollary of great consequence: in the future, CAVD may well be controlled (restrained/reversed) by lifestyle and pharmacogenomics remedies, not unlike atherosclerosis. (As Shakespeare put it, “the wheel has come full circle”: Greek physicians from Hippocrates in the fifth century BC to Galen in the second century AD gave careful and detailed advice on how to follow a healthy diet and lifestyle [110].) Moreover, proper management should entail a comprehensive approach that encompasses not only the aortic valve but also the left ventricle and the systemic arterial system, with their inexorably interdependent morphomechanics and hemodynamics, which underlie inception and evolution of diastolic and systolic dysfunction in CAVD patients.

Oncoming studies will be needed to better and more completely characterize the overall dynamics, encompassing intricate feedback mechanisms involving gene network cascades, specific signaling molecules, including mechanoreceptors and mechanotransducers, and hemodynamic/myocardial stresses. In this context, it should be recognized that the usually profuse complexity of the intricate signaling transduction network and feedback pathways, which are available in the working heart in situ, will render it quite challenging to recapitulate effectively, in an in vitro investigative/analytical setting, all interacting consequential mechanisms that can shape specific morphomechanical stages/outcomes during cardiac hypertrophy. In investigating the pertinent genomics and transcriptomics, post-genomic technologies such as high-throughput genotyping will certainly be of extraordinary importance for collecting the large-scale data on the genetic variations in individual patients and in population samples. In performing such big data studies, following Aristotle’s paradigm, one should always remember that statistical correlation/regression cannot by itself yield causal explanations (understanding) and prediction, although it commonly provides a useful conceptual aid and it can be a solid source of insights. In absence of a cogent, validated theoretical model, however, mere correlation does not imply causation, and one cannot predict what will result from changing either the structure of the population sample or the biochemistry of the individual(s) investigated. Bearing this in mind, our more or less rapidly developing future knowledge will right from the outset be

more or less directly harvestable, allowing us to treat CAVD/AVS in the ageing population—see Epigraphs—rationally and strategically.

Acknowledgments

Sources of Funding

Research support, for work from my Laboratory surveyed here, was provided by: National Heart, Lung, and Blood Institute, Grant R01 HL 050446; National Science Foundation, Grant CDR 8622201; and North Carolina Supercomputing Center and Cray Research.

References

1. Roberts WC, Ko JM. Frequency by decades of unicuspid, bicuspid, and tricuspid aortic valves in adults having isolated aortic valve replacement for aortic stenosis, with or without associated aortic regurgitation. Circulation. 2005; 111:920–5. [PubMed: 15710758]
2. Chambers J. Aortic stenosis. Is common, but often unrecognised (Editorial). BMJ. 2005; 330:801–2. [PubMed: 15817530]
3. Aksoy O, Cam A, Agarwal S, et al. Significance of aortic valve calcification in patients with low-gradient low-flow aortic stenosis. Clin Cardiol. 2014; 37:26–31. [PubMed: 24122890]
4. Pasipoularides A. Mechanotransduction mechanisms for intraventricular diastolic vortex forces and myocardial deformations: Part 1. J Cardiovasc Transl Res. 2015; 8:76–87. [PubMed: 25624114]
5. Pasipoularides A. Mechanotransduction mechanisms for intraventricular diastolic vortex forces and myocardial deformations: Part 2. J Cardiovasc Transl Res. 2015; 8:293–318. [PubMed: 25971844]
6. Rajamannan NM, Evans FJ, Aikawa E, et al. Calcific aortic valve disease: not simply a degenerative process: a review and agenda for research from the National Heart and Lung and Blood Institute Aortic Stenosis Working Group. Executive summary: calcific aortic valve disease–2011 update. Circulation. 2011; 124:1783–91. [PubMed: 22007101]
7. Simmons CA, Grant GR, Manduchi E, Davies PF. Spatial heterogeneity of endothelial phenotypes correlates with side-specific vulnerability to calcification in normal porcine aortic valves. Circ Res. 2005; 96:792–9. [PubMed: 15761200]
8. Alexopoulos A, Bravou V, Peroukides S, Kaklamanis L, Varakis J, Alexopoulos D, Papadaki H. Bone regulatory factors NFATc1 and Osterix in human calcific aortic valves. Int J Cardiol. 2010; 139:142–9. [PubMed: 19019468]
9. Yutzey KE, Demer LL, Body SC, et al. Calcific aortic valve disease: a consensus summary from the Alliance of Investigators on Calcific Aortic Valve Disease. Arterioscler Thromb Vasc Biol. 2014; 34:2387–93. [PubMed: 25189570]
10. Pasipoularides A. Historical continuity in the methodology of modern medical science: Leonardo leads the way. Intern J Cardiol. 2014; 171:103–15.
11. Quiney, JR.; Watts, GB. Introduction. In: Quiney, JR.; Watts, GB., editors. Classic papers in hyperlipidemia. London: Science Press Limited; 1989.
12. Mönckeberg JG. Der normale histologische Bau und die Sklerose der Aortenklappen. Virchows Arch Pathol Anat Physiol. 1904; 176:472–514.
13. Pasipoularides, A. Heart's Vortex: Intracardiac Blood Flow Phenomena. Shelton, CT: People's Medical Publishing House; 2010. p. 960
14. Rajamannan NM. Calcific aortic valve disease: cellular origins of valve calcification. Arterioscler Thromb Vasc Biol. 2011; 31:2777–8. [PubMed: 22096095]
15. Schoen FJ. Evolving concepts of cardiac valve dynamics: the continuum of development, functional structure, pathobiology, and tissue engineering. Circulation. 2008; 118:1864–80. [PubMed: 18955677]
16. Rodriguez KJ, Masters KS. Regulation of valvular interstitial cell calcification by components of the extracellular matrix. J Biomed Mater Res A. 2009; 90:1043–53. [PubMed: 18671262]

17. Yip CY, Chen JH, Zhao R, Simmons CA. Calcification by valve interstitial cells is regulated by the stiffness of the extracellular matrix. Arterioscler Thromb Vasc Biol. 2009; 29:936–42. [PubMed: 19304575]
18. Chen JH, Chen WL, Sider KL, Yip CY, Simmons CA. β-catenin mediates mechanically regulated, transforming growth factor-β1-induced myofibroblast differentiation of aortic valve interstitial cells. Arterioscler Thromb Vasc Biol. 2011; 31:590–7. [PubMed: 21127288]
19. Schoen FJ. Aortic valve structure-function correlations: role of elastic fibers no longer a stretch of the imagination. J Heart Valve Dis. 1997; 6:1–6. [PubMed: 9044068]
20. Rabkin E, Aikawa M, Stone JR, Fukumoto Y, Libby P, Schoen FJ. Activated interstitial myofibroblasts express catabolic enzymes and mediate matrix remodeling in myxomatous heart valves. Circulation. 2001; 104:2525–32. [PubMed: 11714645]
21. Fondard O, Detaint D, Iung B, et al. Extracellular matrix remodelling in human aortic valve disease: the role of matrix metalloproteinases and their tissue inhibitors. Eur Heart J. 2005; 26:1333–41. [PubMed: 15827062]
22. Coffey S, Cox B, Williams MJ. The prevalence, incidence, progression, and risks of aortic valve sclerosis: a systematic review and meta-analysis. J Am Coll Cardiol. 2014; 63:2852–61. [PubMed: 24814496]
23. Cottignoli V, Cavarretta E, Salvador L, Valfré C, Maras A. Morphological and chemical study of pathological deposits in human aortic and mitral valve stenosis: a biomineralogical contribution. Patholog Res Int. 2015; 2015:342984.10.1155/2015/342984 [PubMed: 25685595]
24. Gey C, Giannis A. Small molecules, big plans--can low-molecular-weight compounds control human regeneration? Angew Chem Int Ed Engl. 2004; 43:3998–4000. [PubMed: 15300685]
25. Lee SJ, Lee HK, Cho SY, et al. Identification of osteogenic purmorphamine derivatives. Mol Cells. 2008; 26:380–6. [PubMed: 18695357]
26. Leopold JA. Cellular mechanisms of aortic valve calcification. Circ Cardiovasc Interv. 2012; 5:605–14. [PubMed: 22896576]
27. New SE, Aikawa E. Molecular imaging insights into early inflammatory stages of arterial and aortic valve calcification. Circ Res. 2011; 108:1381–91. [PubMed: 21617135]
28. Dweck MR, Boon NA, Newby DE. Calcific aortic stenosis: a disease of the valve and the myocardium. J Am Coll Cardiol. 2012; 60:1854–63. [PubMed: 23062541]
29. Smith JG, Luk K, Schulz CA, et al. Association of low-density lipoprotein cholesterol-related genetic variants with aortic valve calcium and incident aortic stenosis. JAMA. 2014; 312:1764–71. [PubMed: 25344734]
30. Miller JD, Weiss RM, Serrano KM, et al. Lowering plasma cholesterol levels halts progression of aortic valve disease in mice. Circulation. 2009; 119:2693–701. [PubMed: 19433756]
31. Mathieu P, Poirier P, Pibarot P, Lemieux I, Després JP. Visceral obesity: the link among inflammation, hypertension, and cardiovascular disease. Hypertension. 2009; 53:577–84. [PubMed: 19237685]
32. Mathieu P, Després J, Pibarot P. The “valvulo-metabolic” risk in calcific aortic valve disease. Can J Cardiol. 2007; 23(Suppl B):32B–9B.
33. Caira FC, Stock SR, Gleason TG, et al. Human degenerative valve disease is associated with up-regulation of low-density lipoprotein receptor-related protein 5 receptor-mediated bone formation. J Am Coll Cardiol. 2006; 47:1707–12. [PubMed: 16631011]
34. Mathieu P, Bouchareb R, Boulanger MC. Innate and adaptive immunity in calcific aortic valve disease. J Immunol Res. 2015; 2015:851945.10.1155/2015/851945 [PubMed: 26065007]
35. Rosenhek R, Rader F, Loho N, et al. Statins but not angiotensin-converting enzyme inhibitors delay progression of aortic stenosis. Circulation. 2004; 110:1291–5. [PubMed: 15337704]
36. Helske S, Kupari M, Lindstedt KA, Kovanen PT. Aortic valve stenosis: an active atheroinflammatory process. Curr Opin Lipidol. 2007; 18:483–91. [PubMed: 17885417]
37. Weiss RM, Miller JD, Heistad DD. Fibrocalcific aortic valve disease: opportunity to understand disease mechanisms using mouse models. Circ Res. 2013; 113:209–22. [PubMed: 23833295]
38. Otto CM, O’Brien KD. Why is there discordance between calcific aortic stenosis and coronary artery disease? Heart. 2001; 85:601–2. [PubMed: 11359728]

39. Cowell SJ, Newby DE, Prescott RJ, et al. A randomized trial of intensive lipid-lowering therapy in calcific aortic stenosis. N Engl J Med. 2005; 352:2389–97. [PubMed: 15944423]
40. Chan KL, Teo K, Dumesnil JG, Ni A, Tam J. ASTRONOMER Investigators. Effect of Lipid lowering with rosuvastatin on progression of aortic stenosis: results of the aortic stenosis progression observation: measuring effects of rosuvastatin (ASTRONOMER) trial. Circulation. 2010; 121:306–14. [PubMed: 20048204]
41. Pasipoularides A. Linking genes to cardiovascular diseases: gene action and gene–environment interactions. J Cardiovasc Transl Res. 2015; 8:506–27. [PubMed: 26545598]
42. Evangelou E, Ioannidis JP. Meta-analysis methods for genome-wide association studies and beyond. Nat Rev Genet. 2013; 14:379–89. [PubMed: 23657481]
43. Hindorff LA1, Sethupathy P, Junkins HA, et al. Potential etiologic and functional implications of genome-wide association loci for human diseases and traits. Proc Natl Acad Sci USA. 2009; 106:9362–7. [PubMed: 19474294]
44. Wray NR, Yang J, Hayes BJ, Price AL, Goddard ME, Visscher PM. Pitfalls of predicting complex traits from SNPs. Nat Rev Genet. 2013; 14:507–15. [PubMed: 23774735]
45. Pasipoularides AD, Shu M, Womack MS, Shah A, von Ramm O, Glower DD. RV functional imaging: 3-D echo-derived dynamic geometry and flow field simulations. Am J Physiol: Heart Circ Physiol. 2003; 284:H56–65. [PubMed: 12388220]
46. Cassar DeMarco D, Monaghan MJ. The role of echocardiography in transcatheter aortic valve implantation. Interv Cardiol (Lond). 2014; 6:547–55.
47. Attias D, Macron L, Dreyfus J, et al. Relationship between longitudinal strain and symptomatic status in aortic stenosis. J Am Soc Echocardiogr. 2013; 26:868–74. [PubMed: 23768690]
48. Schueler R, Sinning JM, Momcilovic D, et al. Three-dimensional speckle-tracking analysis of left ventricular function after transcatheter aortic valve implantation. J Am Soc Echocardiogr. 2012; 25:827–34. [PubMed: 22658423]
49. Lang RM, Badano LP, Tsang W, et al. EAE/ASE recommendations for image acquisition and display using three-dimensional echocardiography. J Am Soc Echocardiogr. 2012; 25:3–46. [PubMed: 22183020]
50. Baumgartner H, Hung J, Bermejo J, et al. Echocardiographic assessment of valve stenosis: EAE/ASE recommendations for clinical practice. J Am Soc Echocardiogr. 2009; 22:1–23. [PubMed: 19130998]
51. Ozkan A, Kapadia S, Tuzcu M, Marwick TH. Assessment of left ventricular function in aortic stenosis. Nat Rev Cardiol. 2011; 8:494–501. [PubMed: 21670747]
52. Knebel F, Schimke I, Schroeckh S, et al. Myocardial function in older male amateur marathon runners: assessment by tissue Doppler echocardiography, speckle tracking, and cardiac biomarkers. J Am Soc Echocardiogr. 2009; 22:803–9. [PubMed: 19505796]
53. Pasipoularides A. Right and left ventricular diastolic pressure–volume relations: a comprehensive review. J Cardiovasc Transl Res. 2013; 6:239–52. [PubMed: 23179133]
54. Pasipoularides A. LV twisting and untwisting in HCM: ejection begets filling. Diastolic functional aspects of HCM. Am Heart J. 2011; 162:798–810. [PubMed: 22093194]
55. Baumgartner H, Hung J, Bernejo J, et al. Echocardiographic assessment of valve stenosis: EAE/ASE recommendations for clinical practice. J Am Soc Echocardiogr. 2009; 22:1–23. [PubMed: 19130998]
56. Lloyd TR. Variation in Doppler-derived stenotic aortic valve area during ejection. Am Heart J. 1992:529–32. [PubMed: 1636603]
57. Kasprzak JD, Nosir YF, Dall'Agata A, et al. Quantification of the aortic valve area in three-dimensional echocardiographic data sets: analysis of orifice overestimation resulting from suboptimal cut-plane selection. Am Heart J. 1998; 135:995–1003. [PubMed: 9630103]
58. Ng AC, Delgado V, van der Kley F, et al. Comparison of aortic root dimensions and geometries before and after transcatheter aortic valve implantation by 2- and 3-dimensional transesophageal echocardiography and multislice computed tomography. Circ Cardiovasc Imaging. 2010; 3:94–102. [PubMed: 19920027]
59. Lang RM, Tsang W, Weinert L, Mor-Avi V, Chandra S. Valvular heart disease. The value of 3-dimensional echocardiography. J Am Coll Cardiol. 2011; 58:1933–44. [PubMed: 22032703]

60. Michelena HI, Margaryan E, Miller FA, et al. Inconsistent echocardiographic grading of aortic stenosis: is the left ventricular outflow tract important? Heart. 2013; 99:921–31. [PubMed: 23349350]

61. Bhatia N, Dawn B, Siddiqui TS, et al. Impact and predictors of noncircular left ventricular outflow tract shapes on estimating aortic stenosis severity by means of continuity equations. Tex Heart Inst J. 2015; 42:16–24. [PubMed: 25873793]

62. Pasipoularides A. Clinical assessment of ventricular ejection dynamics with and without outflow obstruction. J Am Coll Cardiol. 1990; 15:859–82. [PubMed: 2407763]

63. Nishimura RA, Otto CM, Bonow RO, et al. 2014 AHA/ACC Guideline for the Management of Patients With Valvular Heart Disease: A Report of the American College of Cardiology/American Heart Association Task Force on Practice Guidelines. J Am Coll Cardiol. 2014; 63:e57–e185. [PubMed: 24603191]

64. Dahl JS, Eleid MF, Pislaru SV, et al. Development of paradoxical low-flow, low-gradient severe aortic stenosis. Heart. 2015; 101:1015–23. [PubMed: 25794516]

65. Barone-Rochette G, Pierard S, Seldrum S, et al. Aortic valve area, stroke volume, left ventricular hypertrophy, remodeling, and fibrosis in aortic stenosis assessed by cardiac magnetic resonance imaging: comparison between high and low gradient and normal and low flow aortic stenosis. Circ Cardiovasc Imaging. 2013; 6:1009–17. [PubMed: 24100045]

66. Clavel MA, Ennezat PV, Marechaux S, et al. Stress echocardiography to assess stenosis severity and predict outcome in patients with paradoxical low-flow, low-gradient aortic stenosis and preserved LVEF. JACC Cardiovasc Imaging. 2013; 6:175–83. [PubMed: 23489531]

67. Tribouilloy C, Rusinaru D, Marechaux S, et al. Low-gradient, low-flow severe aortic stenosis with preserved left ventricular ejection fraction: characteristics, outcome, and implications for surgery. J Am Coll Cardiol. 2015; 65:55–66. [PubMed: 25572511]

68. Hachicha Z, Dumesnil JG, Bogaty P, Pibarot P. Paradoxical low-flow, low-gradient severe aortic stenosis despite preserved ejection fraction is associated with higher afterload and reduced survival. Circulation. 2007; 115:2856–64. [PubMed: 17533183]

69. Clavel MA, Fuchs C, Burwash IG, et al. Predictors of outcomes in low-flow, low-gradient aortic stenosis: results of the multicenter TOPAS Study. Circulation. 2008; 118(14 Suppl):S234–42. [PubMed: 18824760]

70. Blais C, Burwash IG, Mundigler G, et al. Projected valve area at normal flow rate improves the assessment of stenosis severity in patients with low-flow, low-gradient aortic stenosis: the multicenter TOPAS (Truly or Pseudo-Severe Aortic Stenosis) study. Circulation. 2006; 113:711–21. [PubMed: 16461844]

71. Magne J, Lancellotti P, Piérard LA. Exercise testing in asymptomatic severe aortic stenosis. JACC Cardiovasc Imaging. 2014; 7:188–99. [PubMed: 24524744]

72. Gomez M, Ble M, Cladellas M, et al. Effect of correction of anemia on echocardiographic and clinical parameters in patients with aortic stenosis involving a three-cuspid aortic valve and normal left ventricular ejection fraction. Am J Cardiol. 2015; 116:270–4. [PubMed: 25983280]

73. Pawade TA, Newby DE, Dweck MR. Calcification in aortic stenosis. J Am Coll Cardiol. 2015; 66:561–77. [PubMed: 26227196]

74. Pasipoularides A, Murgo JP, Bird JJ, Craig WE. Fluid dynamics of aortic stenosis: mechanisms for the presence of subvalvular pressure gradients. Am J Physiol: Heart Circ Physiol. 1984; 246:H542–H550.

75. Pasipoularides A, Murgo JP, Miller JW, Craig WE. Nonobstructive left ventricular ejection pressure gradients in man. Circ Res. 1987; 61:220–7. [PubMed: 3621488]

76. Pasipoularides A. Complementarity and competitiveness of the intrinsic and extrinsic components of the total ventricular load: demonstration after valve replacement in aortic stenosis. Am Heart J. 2007; 153:4–6. [PubMed: 17174626]

77. Isaaz K, Pasipoularides A. Noninvasive assessment of intrinsic ventricular load dynamics in dilated cardiomyopathy. J Am Coll Cardiol. 1991; 17:112–21. [PubMed: 1987212]

78. Pasipoularides A. Cardiac mechanics: basic and clinical contemporary research. Ann Biomed Eng. 1992; 20:3–17. [PubMed: 1562103]

79. Pasipoularides A. Fluid dynamic aspects of ejection in hypertrophic cardiomyopathy. Hellenic J Cardiol. 2011; 52:416–26. [PubMed: 21940289]
80. Laskey WK, Kussmaul WG. Subvalvular gradients in patients with valvular aortic stenosis: prevalence, magnitude, and physiological importance. Circulation. 2001; 104:1019–22. [PubMed: 11524395]
81. Schöbel WA, Voelker W, Haase KK, Karsch K-R. Extent, determinants and clinical importance of pressure recovery in patients with aortic valve stenosis. Eur Heart J. 1999; 20:1355–63. [PubMed: 10462470]
82. Pasipoularides A. Right and left ventricular diastolic flow field: why are measured intraventricular pressure gradients small? Rev Esp Cardiol. 2013; 66:337–41. [PubMed: 24775813]
83. Bird JJ, Murgo JP, Pasipoularides A. Fluid dynamics of aortic stenosis: Subvalvular gradients without subvalvular obstruction. Circulation. 1982; 66:835–40. [PubMed: 6889475]
84. Georgiadis JG, Wang M, Pasipoularides A. Computational fluid dynamics of left ventricular ejection. Ann Biomed Eng. 1992; 20:81–97. [PubMed: 1562106]
85. Hampton T, Shim Y, Straley C, Pasipoularides A. Finite element analysis of cardiac ejection dynamics: Ultrasonic implications. Am Soc Mechan Engin, Bioengin Div (ASME BED) Adv Bioengin. 1992; 22:371–4.
86. Hampton T, Shim Y, Straley C, Uppal R, Smith PK, Glower D, Pasipoularides A. Computational fluid dynamics of ventricular ejection on the CRAY Y-MP. IEEE Proc Comp Cardiol. 1992; 19:295–8.
87. Pasipoularides A, Murgo JP, Bird JJ, Craig WE. Fluid dynamics of aortic stenosis: Mechanisms for the presence of subvalvular pressure gradients. Am J Physiol. 1984; 246:H542–50. [PubMed: 6720911]
88. Barki-Harrington L, Perrino C, Rockman HA. Network integration of the adrenergic system in cardiac hypertrophy. Cardiovasc Res. 2004; 63:391–402. [PubMed: 15276464]
89. Mann DL, Kent RL, Cooper G. Load regulation of the properties of adult feline cardiocytes: growth induction by cellular deformation. Circ Res. 1989; 64:1079–90. [PubMed: 2470528]
90. Sadoshima J, Izumo S. The cellular and molecular response of cardiac myocytes to mechanical stress. Annu Rev Physiol. 1997; 59:551–71. [PubMed: 9074777]
91. Yamazaki T, Komuro I, Nagai R, Yazaki Y. Stretching the evidence in the case of cardiac growth. Cardiovasc Res. 1996; 31:493–8. [PubMed: 9138859]
92. Wee KB, Yio WK, Surana U, Chiam KH. Transcription factor oscillations induce differential gene expressions. Biophys J. 2012; 102:2413–23. [PubMed: 22713556]
93. Guyton AC, Crowell JW, Moore JW. Basic oscillating mechanism of Cheyne-Stokes breathing. Amer J Physiol. 1956; 187:395–8. [PubMed: 13372802]
94. Paulus WJ, Grossman W, Serizawa T, Bourdillon PD, Pasipoularides A, Mirsky I. Different effects of two types of ischemia on myocardial systolic and diastolic function. Am J Physiol Heart Circ Physiol. 1985; 248:H719–28.
95. Pasipoularides A, Palacios I, Frist W, Rosenthal S, Newell JB, Powell WJ Jr. Contribution of activation-inactivation dynamics to the impairment of relaxation in hypoxic cat papillary muscle. Am J Physiol Regulatory Integrative Comp Physiol. 1985; 248:R54–62.
96. Gelpi RJ, Pasipoularides A, Lader AS, Patrick TA, Chase N, Hittinger L, Shannon RP, Bishop SP, Vatner SF. Changes in diastolic cardiac function in developing and stable perinephritic hypertension in conscious dogs. Circ Res. 1991; 68:555–67. [PubMed: 1991355]
97. Komamura K, Shannon RP, Pasipoularides A, Ihara T, Lader AS, Patrick TA, Bishop SP, Vatner SF. Alterations in left ventricular diastolic function in conscious dogs with pacing-induced heart failure. J Clin Invest. 1992; 89:1825–38. [PubMed: 1601992]
98. Pasipoularides A, Mirsky I, Hess OM, Grimm J, Krayenbuehl HP. Muscle relaxation and passive diastolic properties in man. Circulation. 1986; 74:991–1001. [PubMed: 3769181]
99. Mirsky I, Pasipoularides A. Clinical assessment of diastolic function. Prog Cardiovasc Dis. 1990; 32:291–318. [PubMed: 2405455]
100. Mirsky I, Pasipoularides A. Elastic properties of normal and hypertrophied cardiac muscle. Federation Proc. 1980; 39:156–61. [PubMed: 6444389]

101. Laks MM, Garner D, Swan HJC. Volumes and compliances measured simultaneously in the right and left ventricle of dog. Circ Res. 1967; 20:565–9. [PubMed: 6057689]

102. Laks MM, Morady F, Garner D, Swan HJC. Relation of ventricular volume, compliance and mass in the normal and pulmonary arterial banded canine heart. Cardiovasc Res. 1972; 6:187–98. [PubMed: 4260766]

103. Laks MM, Morady F. Norepinephrine—the myocardial hypertrophy hormone? Am Heart J. 1976; 91:674–5. [PubMed: 131482]

104. Moss RL, Fitzsimons DP. Regulation of contraction in mammalian striated muscles—the plot thickens. J Gen Physiol. 2010; 136:21–7. [PubMed: 20584889]

105. Solaro RJ, Sheehan KA, Lei M, Ke YB. The curious role of sarcomeric proteins in control of diverse processes in cardiac myocytes. J Gen Physiol. 2010; 136:13–9. [PubMed: 20584888]

106. Pal PD, Dongre PM, Chitre AV. “Is macromolecular crowding overlooked?”--Effects of volume exclusion on DNA-amino acids complexes and their reconstitutes. J Fluoresc. 2014; 24:1275–84. [PubMed: 24894381]

107. Kinjo AR, Takada S. Competition between protein folding and aggregation with molecular chaperones in crowded solutions: insight from mesoscopic simulations. Biophys J. 2003; 85:3521–31. [PubMed: 14645047]

108. Bernadó P, García de la Torre J, Pons M. Macromolecular crowding in biological systems: hydrodynamics and NMR methods. J Mol Recognit. 2004; 17:397–407. [PubMed: 15362098]

109. Ellis RJ, Minton AP. Protein aggregation in crowded environments. Biol Chem. 2006; 387:485–97. [PubMed: 16740119]

110. Pasipoularides, A. Galen, father of systematic medicine. An essay on the evolution of modern medicine and cardiology. Int J Cardiol. 2014; 172:47–58. [PubMed: 24461486]

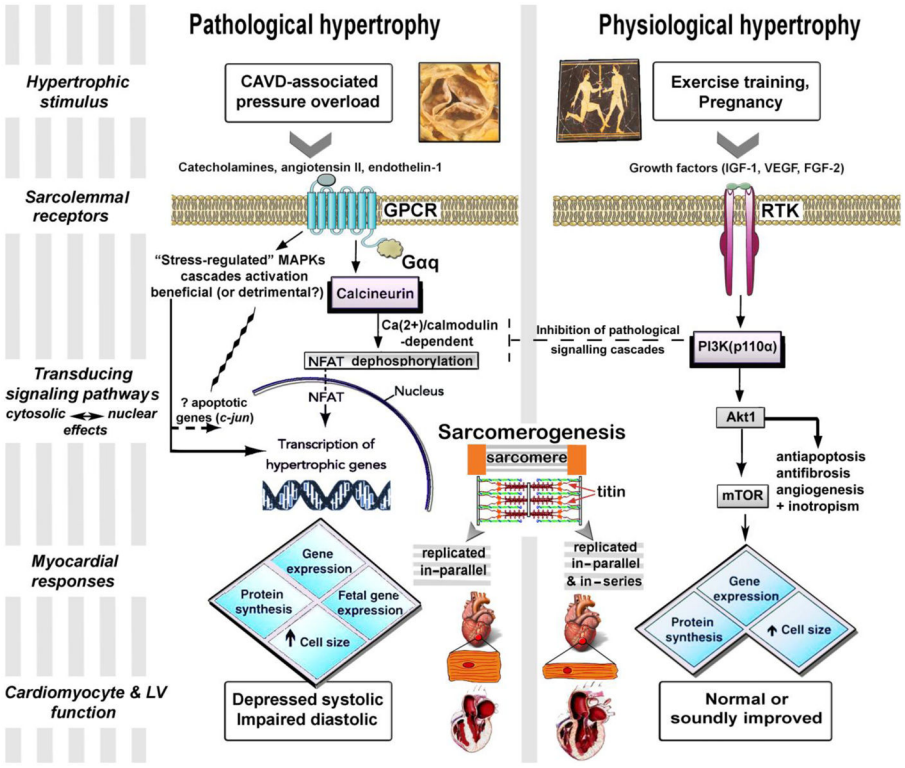

Fig 1.

Pathways involved in physiological and in pathological cardiac hypertrophy actuated in calcific aortic valve disease (CAVD). Signal transduction pathways pave the way for cellular mechanisms controlling gene expression; a cascade of molecules leading to the activation of one or more specific transcription factors is actuated. The extracellular signals in the form of ligands/effector molecules, which bind to specific receptors to initiate the hypertrophy producing pathways, are transcribed across the sarcolemma via an assortment of second messengers. In physiological forms of cardiomyocyte/myocardial growth only direct mechanotransduction routes and the PI3K(p110α) lipid kinase - Akt serine/threonine kinase pathway are activated, downstream from receptor tyrosine kinases (RTK), leading to left ventricular (LV) remodeling involving replication of cardiomyocyte sarcomeres both in-parallel and in-series and an eccentric LV hypertrophy pattern with enhanced myocardial performance. On the other hand, in the pathological form of hypertrophy that is induced in conjunction with the LV pressure overload of CAVD (or hypertension), there ensues activation of a diverse, wider variety of signaling pathways, involving G Protein-Coupled Receptors (GPCR). GPCR mediate pathological cardiac hypertrophy through downstream mitogen-activated protein kinases (MAPKs) such as extracellular signal-regulated kinases 1 and 2 (ERK1/2), and calcineurin, a Ca^{2+}-dependent phosphatase that controls hypertrophic gene transcription by dephosphorylating transcription factors such as nuclear factor of activated T-cells (NFAT). This ultimately leads to the identifiable expression of a maladaptive genetic program, with activation of protein translation concluding with replication of cardiomyocyte sarcomeres in-parallel and a typically concentric LV hypertrophy; these are complicated by cellular apoptosis and ECM fibrosis, by

(subendocardial) ischemia with diastolic and systolic dysfunction, and by transition to heart failure with subsequent LV chamber dilatation (see particulars in text).

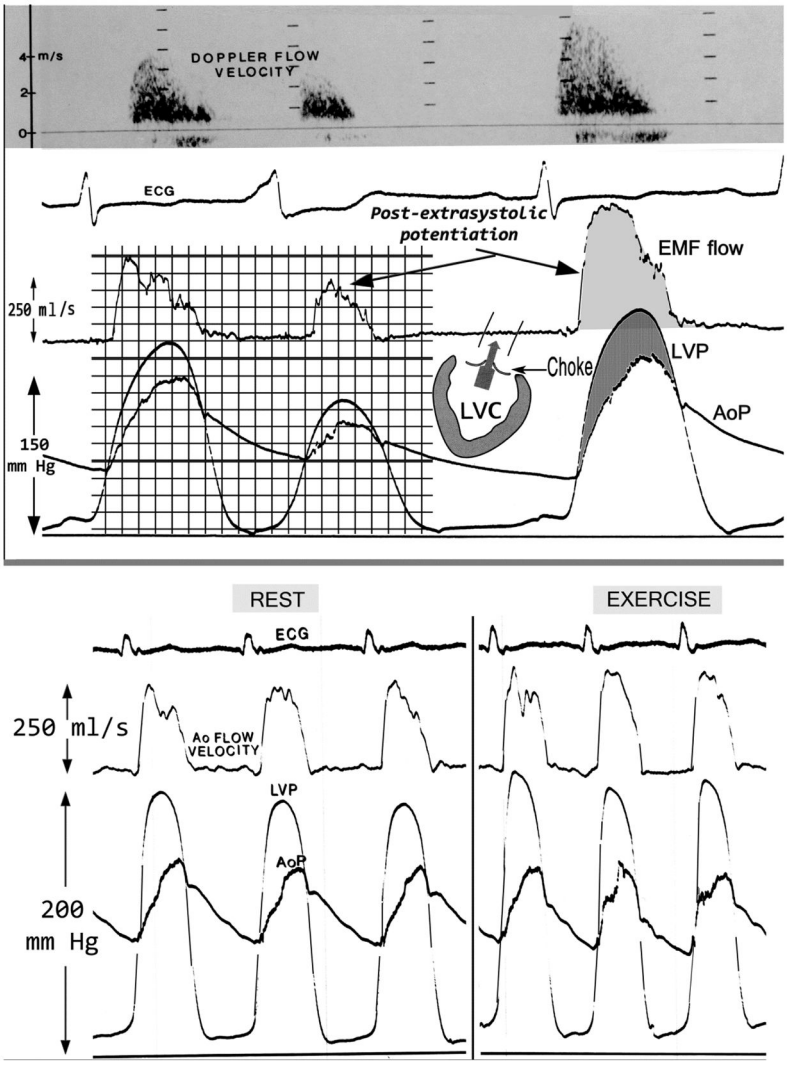

Fig 2.

Top panels: In a patient with AVS, the congruence in the simultaneously measured flow waveform shapes by transthoracic continuous wave Doppler (CWD) and by an intravascular catheter-mounted electromagnetic flowmeter (EMF) probe is striking. *Bottom panels*: The marked dependence of the flow-driving pressure gradient values on the matching flow velocities is clear. The high frequency fluctuations on the downstroke of the aortic root EMF velocity waveforms and on the aortic root systolic pressure tracing in AVS are characteristic of the inception of turbulence—decelerating flows are relatively unstable, as a rule, whereas accelerating flows (upstroke) tend to be more stable. These fluctuations tend to be more prominent during even a modest intensity exercise, because of the rise in turbulence intensity ensuing with the higher transvalvular ejection velocities. LV = left ventricular; Ao = aortic; C = chamber; P = pressure. Adapted with permission of PMPH-USA from Pasipoularides A. *Heart's Vortex: Intracardiac Blood Flow Phenomena* [13].

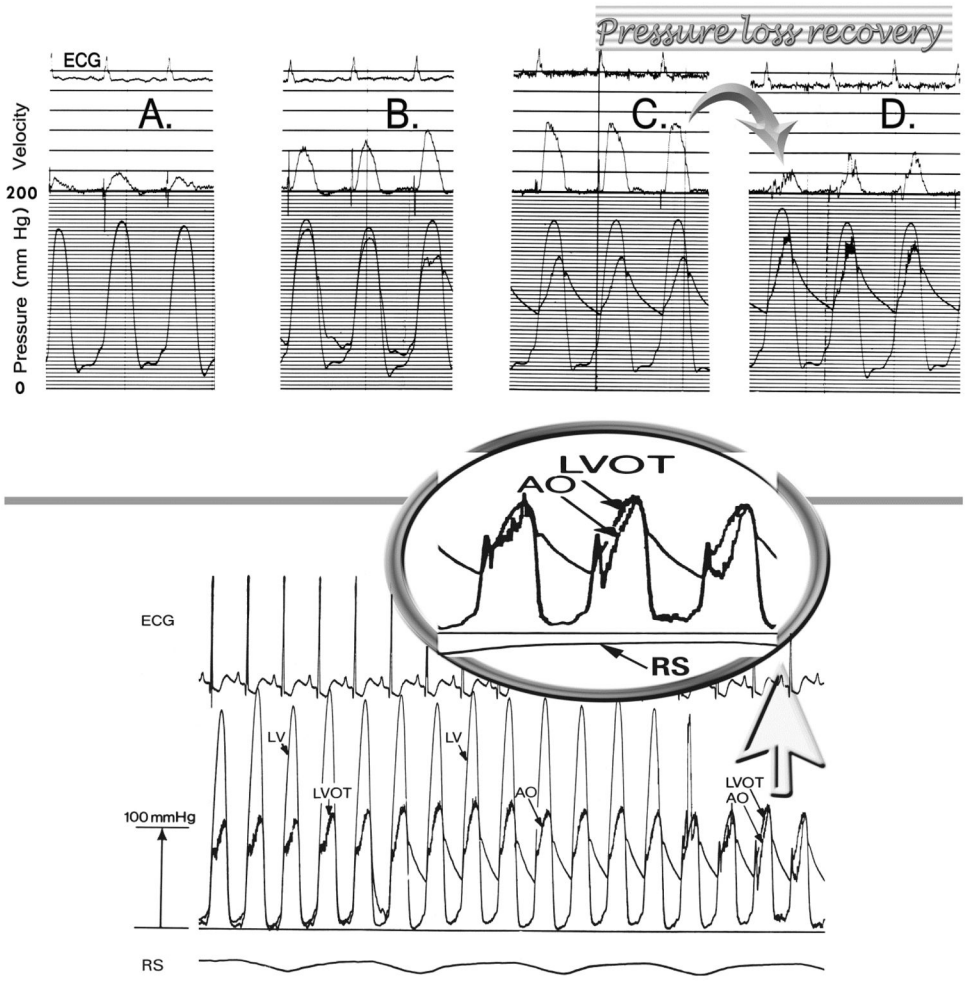

Fig 3.

Top panels: Multisensor catheter pullback in AVS, performed utilizing a left-heart solid-state multisensor Millar catheter (Millar Instruments, Houston, TX) with 2 laterally mounted micromanometers, one at the catheter tip and the second 5 cm proximal to the first and an electromagnetic flow velocity probe at the level of the proximal micromanometer, demonstrating both the strong increase in the subvalvular flow velocity that is associated with the large measured subvalvular pressure gradient just upstream of the stenosed orifice and the pressure loss recovery in the ascending aorta (see text discussion). From top downward: electrocardiogram; linear velocity in deep chamber (panel A), subvalvular region (panel B), vena contracta (panel C) and dilated ascending aorta (panel D); distal and proximal micromanometric signals. *Bottom panel*: Micromanometric signals obtained by a left-heart Millar “double-tip” catheter—5 cm distance between the 2 micromanometers—during multisensor catheter pullback revealing that the “transvalvular” pressure gradient in AVS is, nearly in its entirety, *intraventricular* in origin: “magnifying lens” inset (see text discussion). AO = aortic root pressure; LV = deep left ventricular pressure; LVOT= left ventricular outflow tract pressure; ECG = electrocardiogram; RS = respiration signal. Top panels, slightly modified from Pasipoularides [62] with permission of the American College

of Cardiology. Bottom panel, reproduced with permission of PMPH-USA from Pasipoularides A. *Heart's Vortex: Intracardiac Blood Flow Phenomena* [13].

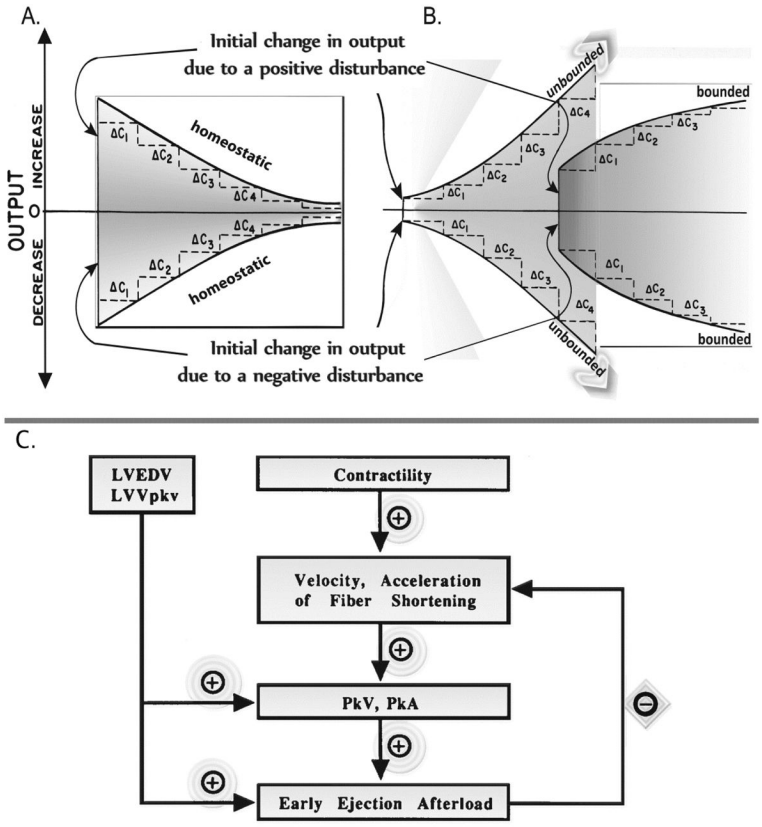

Fig 4.

A feedback loop generally comprises a chain of actions (*a, b, c*…) where *a* modifies or influences *b*, then *b* influences *c*, and so on until ultimately some *x* circles back around to modify *a*. In a “negative” feedback loop, the end result of the chain of influences is that the system as a whole tends to stabilize around an equilibrium position; if the system starts to deviate one way or the other, the feedback loop tends to pull it back toward equilibrium through end-product/end-state activation or inhibition. In a “positive” feedback loop, the end result of the chain of influences is that over time the system as a whole moves away from equilibrium, in one direction or another, toward an abnormal condition. *Top panels*: The output of a negative feedback control system might appear as shown in panel A. In this case, the ratios of successive to preceding values $\Delta C_2/\Delta C_1$, $\Delta C_3/\Delta C_2$, etc., of the controlled variable C(t) are less than unity. Positive feedback may cause what is known as a vicious cycle, or it may not, depending upon the characteristics of the system, as is exemplified in panel B. In the case of the vicious cycle (unbounded response), the ratios $\Delta C_2/\Delta C_1$, $\Delta C_3/\Delta C_2$, etc., are greater than unity. When the response does not result in a vicious cycle (bounded response), the ratios $\Delta C_2/\Delta C_1$, $\Delta C_3/\Delta C_2$, etc., are less than unity. *Bottom panel*: Diagrammatic representation of the interrelation between contractility, load on the ventricular myocardium and ejection variables. Note the negative feedback between the early ejection afterload and the peak velocity and acceleration of the ventricular myocardial fibers. LVEDV = left ventricular end-diastolic volume; LVVpkv = left ventricular volume at the time of peak velocity: PkA = peak outflow acceleration: PkV = peak ejection velocity. Panels A & B, reproduced with permission of PMPH-USA from Pasipoularides A. *Heart's*

Vortex: Intracardiac Blood Flow Phenomena [13] ; panel C, adapted from Isaaz and Pasipoularides [77], by permission of the American College of Cardiology.

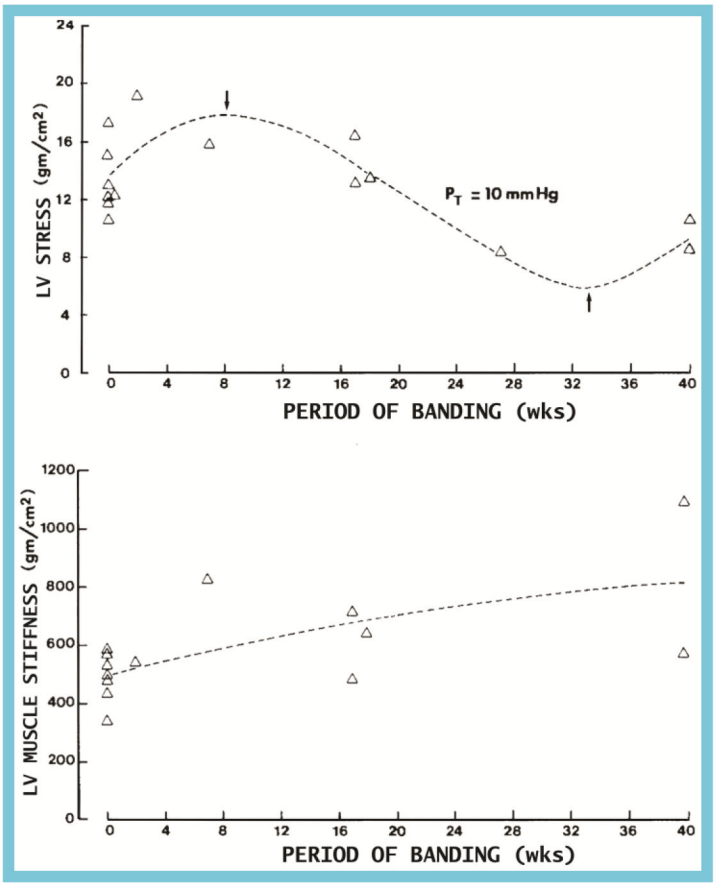

Fig 5.

LV distending wall stress at 10 mm Hg transmural pressure, P_T, (*top*) and LV muscle stiffness at 20 g/cm^2 distending wall stress (*bottom*) plotted as a function of banding period in dog hearts. Observe the early increases in both stress and stiffness before substantial wall mass increase, and the oscillatory behavior of the wall stress—note the long quasi-periodicity, extending over many weeks—with the possibility of normal wall stresses occurring at 3 different times during hypertrophy and incipient heart failure; the system seems to oscillate about its desired normal wall stress goal. Such oscillatory behavior is inherent in any feedback regulatory process. It is referable to the inescapable fact that information delivered by any regulatory feedback loop—subserving homeostatic maintenance of developed cardiomyocyte systolic stress levels within the normal range—can affect only future behavior. It cannot deliver a signal fast enough to correct the behavior/factor that drove the current feedback signal, and using *dated* information to control the approach to a target systolic stress level is likely to cause the system to miss or overshoot/undershoot its goal. There are necessary delays involved in signal transmission and in implementing corrective measures—i.e., replication of sarcomeres in parallel to adjust the systolic stress level—that may overshoot and undershoot their target (see text discussion). Figure adapted from Mirsky and Pasipoularides [100], by permission of the Federation of American Societies for Experimental Biology.